Electronic Supplementary Information

Propargylated cello-oligosaccharide nanosheets: a water-dispersible, antibiofouling, and post-functionalizable solid support for immunoassays

Kai Sugiura[a], Yuuki Hata[a], Koichiro Ishibashi[b], Toshiki Sawada[a], Hiroshi Tanaka[a,c], Go Watanabe[b,d,e] and Takeshi Serizawa[a,*]

[a] Department of Chemical Science and Engineering, School of Materials and Chemical Technology, Institute of Science Tokyo, 2-12-1 Ookayama, Meguro-ku, Tokyo 152-8550, Japan

[b] Department of Physics, School of Science, Kitasato University, 1-15-1 Kitazato, Minami-ku, Sagamihara, Kanagawa 252-0373, Japan

[c] Faculty of Pharmacy, Juntendo University, 6-8-1 Hinode, Urayasu, Chiba 279-0013, Japan

[d] Department of Data Science, School of Frontier Engineering, Kitasato University, 1-15-1 Kitazato, Minami-ku, Sagamihara, Kanagawa 252-0373, Japan

[e] Kanagawa Institute of Industrial Science and Technology (KISTEC), 705-1 Shimoizumi, Ebina, Kanagawa 243-0435, Japan

* Corresponding author.
E-mail address: serizawa@mct.isct.ac.jp (T. Serizawa)

Contents

Materials and methods

Materials

Sodium methoxide (>95%), strong acidic cation exchange resin (50Wx4 200–400 mesh (H Form)), and bovine serum albumin (BSA, 98%, protease free) were purchased from FUJIFILM Wako Pure Chemical Corporation (Osaka, Japan). *β*-D-Glucose pentaacetate (>99%), boron trifluoride diethyl ether complex (>98%), *p*-anisaldehyde (>99%), and one-terminal methoxy oligo(ethylene glycol)s (OEGs) bearing an azido group at the other terminus with 3, 7, 11, and 23 EG units (mEG_3-N_3, >98%, mEG_7-N_3, >90%, mEG_{11}-N_3, >98%, and mEG_{23}-N_3, >95%, respectively) were purchased from Tokyo Chemical Industry (Tokyo, Japan). 2-Propyn-1-ol (>99%), one-terminal hydroxy OEG bearing an azido group at the other terminus with seven EG units (EG_7-N_3, >95%), and horseradish peroxidase (HRP)-conjugated anti-mouse immunoglobulin G (IgG) antibody (IgG, produced in rabbit, polyclonal, A9044, Lot No. 0000143670) were purchased from Sigma–Aldrich (Missouri, USA). A thin-layer chromatography silica gel plate (60 F254), poly(vinylidene fluoride) membrane filter (Millex-GV, 0.22 μm pore size), anti-poly(ethylene glycol) (PEG) antibody clone 15-2b (IgG, produced in mice, monoclonal, MABS2002-100UG, Lot No. Q3143813), and anti-PEG antibody clone 6.3 (IgG, produced in mice, monoclonal, MABS1966-100UG, Lot No. 3831390) were purchased from Merck Millipore (Massachusetts, USA). Anti-PEG antibody clone PEG-B-47 (IgG, produced in rabbits, monoclonal, ab51257, Lot No. GR3297029-4) was purchased from Abcam (Cambridge, United Kingdom). HRP-conjugated anti-rabbit IgG antibody (IgG, produced in goat, polyclonal, GTX213110-01, Lot No. 43607) was purchased from GeneTex (California, USA). Fetal bovine serum was purchased from BioWest (Nuaillé, France) and subjected to heat treatment at 56 °C for 30 min to inactivate complement proteins before use. All other reagents were purchased from Nacalai Tesque (Kyoto, Japan). Dry dichloromethane (DCM) and tetrahydrofuran (THF) were obtained using a Glass Contour solvent purification system (Nikko Hansen, Osaka, Japan). 96-Well plates (clear, flat bottoms) were purchased from Corning (New York, USA). A polypropylene tube (0.2 mL) was purchased from WATSON Bio Lab (Tokyo, Japan). Dotite was purchased from Nissin EM (Tokyo, Japan). Ultrapure water (more than 18.2 MΩ·cm) was obtained from a Milli-Q Advantage A-10 system (Merck Millipore, Massachusetts, USA) and used throughout the study.

Synthesis of propargyl *β*-D-glucopyranoside

Propargyl *β*-D-glucopyranoside primers were synthesized in two steps, as shown in Scheme S1. Boron trifluoride diethyl ether complex (5 equiv.) was added to a mixture of *β*-D-glucose pentaacetate (1 equiv.) and 2-propyn-1-ol (5 equiv.) in dry DCM at 4 °C under an argon atmosphere. After stirring overnight at room temperature, the reaction solution was added to a mixture of a saturated sodium hydrogen carbonate aqueous solution and ethyl acetate to quench the reaction. The extracted organic layer was washed twice with brine and dried using sodium

sulfate. After filtration through a glass filter, the solution was concentrated *in vacuo*. The residue was purified using silica gel column chromatography (10–35% acetone in hexane) and dried *in vacuo*. The residue was further purified by recrystallization from a mixture of ethyl acetate and hexane to provide propargyl 2,3,4,6-tetra-*O*-acetyl-*β*-D-glucopyranoside as a colorless powder in 13% yield. Then, sodium methoxide (0.1 equiv.) was added to a solution of propargyl 2,3,4,6-tetra-*O*-acetyl-*β*-D-glucopyranoside in a mixture of methanol (MeOH) and THF (1/1, v/v) at 4 °C. After stirring overnight at room temperature, a strong acidic cation exchange resin was added to the reaction solution. After filtration through a celite pad, the filtrate was concentrated *in vacuo* to obtain propargyl *β*-D-glucopyranoside as a colorless oil in 90% yield. The solution of propargyl *β*-D-glucopyranoside in water was passed through a polyvinylidene fluoride membrane filter (Millex-GV, 0.22 μm pore size). To monitor all the reactions, thin-layer chromatography was performed and visualized using a silica gel plate and an ethanol solution of *p*-anisaldehyde and hydrogen sulfate. The characterizations of the synthesized compounds are described below.

Enzyme-catalyzed synthesis of propargylated cello-oligosaccharide nanosheets

Cellodextrin phosphorylase-catalyzed oligomerization reactions were performed according to the procedure described in our previous report on the synthesis of aminated cello-oligosaccharides.[1] Briefly, *α*-D-glucose 1-phosphate monomers (200 mM), propargyl *β*-D-glucopyranoside primers (50 mM), and cellodextrin phosphorylase (1 U mL^{-1}, derived from *Acetivibrio thermocellus* DSM 1313) were incubated in 500 mM 4-(2-hydroxyethyl)-1-piperazineethanesulfonic acid buffer solution (pH 7.5) containing 50 μM ethylenediaminetetraacetic acid at 60 °C for 3 d. The water-insoluble products were washed with ultrapure water through centrifugation (20,400 *g*, 4 °C, 10 min) and redispersion cycles to remove at least 99.999% of the reaction solution. The obtained products were dispersed in ultrapure water and stored at 4 °C before use for matrix-assisted laser desorption ionization time-of-flight (MALDI-TOF) mass spectrometry and atomic force microscopy (AFM) observation. For ^{1}H nuclear magnetic resonance (^{1}H NMR) spectroscopy, X-ray diffraction (XRD) measurements, and attenuated total reflection-Fourier transform infrared (ATR-FTIR) absorption spectroscopy, the dispersions were lyophilized. For scanning electron microscopy (SEM) observation, the as-prepared hydrogel products were soaked overnight in ultrapure water at 4 °C. Subsequently, the water was exchanged. This cycle was repeated seven times to remove water-soluble substances from the hydrogels.

Post-functionalization of propargylated cello-oligosaccharide nanosheets

To perform copper(I)-catalyzed azide-alkyne cycloaddition reactions, aqueous solutions of copper(II) sulfate and sodium ascorbate were added in this order to a mixture of propargylated cello-oligosaccharide nanosheets and mEG_n-N_3 or EG_7-N_3 in a water–dimethyl sulfoxide

mixture (1/1, v/v). The final concentrations of the reagents are listed in Table S1. After stirring at 25 °C for 1 h, the insoluble products were washed with ultrapure water through centrifugation (20,400 *g*, 4 °C, 5 min) and redispersion cycles to remove at least 99.999% of the reaction solution. The purified aqueous dispersions were stored at 4 °C before use for MALDI-TOF mass spectrometry, AFM observation, and enzyme-linked immunosorbent assay (ELISA). For ATR-FTIR absorption spectroscopy, the aqueous dispersions were lyophilized.

^{1}H NMR spectroscopy

An AVANCE III HD500 instrument (500 MHz, Bruker Biospin, Massachusetts, USA) was used to record ^{1}H NMR spectrum of propargylated cello-oligosaccharides at > 2% (w/v) in 4% sodium deuteroxide–deuterium oxide solutions under ambient conditions. The spectrum was calibrated using the peak (δ = 4.79) of water as an internal reference.

MALDI-TOF mass spectrometry

An AXIMA Performance instrument (Shimadzu, Kyoto, Japan) equipped with a nitrogen laser (λ = 337 nm) and pulsed ion extraction was used in linear positive mode to acquire the spectra, following calibration with Bradykinin (757.3997 Da), $P_{14}R$ (1533.8582 Da), and ACTH (2465.1989 Da). For sample preparation, mixtures containing cello-oligosaccharides (0.01% (w/v)), 2,5-dihydroxybenzoic acid (2 mg mL^{-1}), and trifluoroacetic acid (0.5 mM) in an acetonitrile–water mixture (1/1, v/v) were deposited onto a sample target plate and dried overnight under ambient conditions before the measurements.

XRD measurement

A MiniFlex600 instrument (Rigaku, Tokyo, Japan) with Cu Kα radiation (λ = 0.154 nm) was used to obtain an XRD profile of the lyophilized product under ambient conditions.

ATR-FTIR spectroscopy

An FT/IR-4100 instrument (JASCO, Tokyo, Japan) equipped with an ATR PRO 450-S accessory (JASCO, Tokyo, Japan) was used to obtain ATR-FTIR absorption spectra of the lyophilized products at a cumulative number of 100 and a resolution of 2.0 cm^{-1} under ambient conditions.

AFM observation

An SPM-9700HT instrument (Shimadzu, Kyoto, Japan) was used to obtain AFM images in the tapping mode under ambient conditions. The samples were prepared by spin-casting water-dispersions of 0.001% (w/v) nanosheets on mica at 600 rpm for 30 min.

The heights (h) of OEG layer were estimated based on the following equation:

$$h = (f/0.65\ (nm^2)) \times 10^{14}/(N_A) \times 367.46\ (g/mol)/1.12\ (g/cm^3) \times 10^7 \quad (1)$$

where 0.65 (nm^2) is the unit cell area of the cellulose II crystal lattice,[2] f is mEG_7 conjugation rate, 367.46 (g/mol) is molecular weight of mEG_7 moiety, and 1.12 (g/cm^3)[3] is density of heptaethylene glycol.

SEM observation

A JSM-7500F instrument (JEOL, Tokyo, Japan) was used to obtain SEM images at an accelerating voltage of 5 kV. To prepare the samples, ultrapure water in the purified hydrogels was gradually exchanged by immersing the gels in 10, 20, 30, 40, 50, 60, 70, 80, and 90% ethanol, ethanol (three times), an ethanol–*tert*-butyl alcohol mixture (1/1, v/v), and then *tert*-butyl alcohol (three times) for 15 min each. The prepared organogels were frozen in liquid nitrogen, cut using a razor blade, and lyophilized. The resulting dried gels were placed on a sample stage using Dotite, with the cut area of the gel facing upward, and dried for 2 h. Then, the samples were coated with osmium using a Neoc-Pro osmium coater (Meiwafosis, Tokyo, Japan) at 5 mA for 60 s.

Dispersion stability test

Aqueous dispersions of nanosheets at 0.5% (w/v) in phosphate-buffered saline (PBS, 137 mM NaCl, pH 7.4) were prepared. The dispersions in a vial were gently stirred by pipetting before incubation for 1 h under ambient conditions.

Adsorption of BSA onto propargylated cello-oligosaccharide nanosheets

Aqueous dispersions of propargylated cello-oligosaccharide nanosheets in PBS were mixed with BSA solutions in PBS. The final concentrations of the propargylated cello-oligosaccharide nanosheets and BSA were 0.2% (w/v) and 20 μM (0.134% (w/v)), respectively. After incubation at 25 °C for 1 h, the mixtures were centrifuged (20,400 *g*, 15 min, 25 °C) to precipitate propargylated cello-oligosaccharide nanosheets and obtain supernatants. A V-670 instrument (JASCO, Tokyo, Japan) was used to record ultraviolet-visible absorption spectra of the supernatants under ambient conditions. The BSA concentration in the supernatant was determined from the absorbance at 280 nm using a calibration curve. The difference of concentration between in the supernatant and in the initial BSA concentration was used to calculate the amount of BSA adsorbed onto the propargylated nanosheets. These experiments were performed with three replicates. BSA adsorption amount per unit surface area (ng cm^{-2}) was calculated using the unit cell area of the cellulose II crystal lattice (0.65 nm^2 per single cello-oligosaccharide chain), as performed in our previous studies.[4,5]

ELISAs of monoclonal anti-PEG antibodies

The OEG-conjugated cello-oligosaccharide nanosheets with conjugation rates of 7–10% were used, unless otherwise stated. ELISAs were performed according to the methods described in our previous report.[4] Ten microliters of 0.5% (w/v) nanosheet dispersions in PBS was mixed with 100 μL of anti-PEG antibody solutions (11 ng mL^{-1}, 110 ng mL^{-1}, and 220 ng mL^{-1} for PEG-B-47, 15-2b, and 6.3, respectively) in PBS containing 3.3% (w/v) BSA in polypropylene tubes. After incubation at 25 °C for 1 h, the mixtures were centrifuged (20,400 *g*, 5 min, 25 °C), and 100 μL of the supernatant was removed. Then, 100 μL of PBS was added to the precipitates to redisperse them. This washing cycle was repeated three times. One hundred microliters of 440 ng mL^{-1} HRP-conjugated anti-IgG antibody solution in PBS containing 3.3% (w/v) BSA was added to the precipitates to disperse them. After incubation at 25 °C for 1 h, the mixtures were centrifuged (20,400 *g*, 5 min, 25 °C), and 100 μL of the supernatant was removed. The same washing cycle was repeated three times. To the precipitates, 2 mg mL^{-1} *o*-phenylenediamine solution in a McIlvaine buffer solution at pH 4.0 containing 0.1% (w/v) hydrogen peroxide was added to initiate the HRP-catalyzed reactions at 25 °C for 30 min. The reactions were quenched by adding 100 μL of 1.5 M sulfuric acid aqueous solution. Then, the reaction solutions were centrifuged (20,400 *g*, 15 min, 25 °C) to precipitate nanosheets, and 100 μL of each supernatant was added to a well of a 96-well plate. The absorbance of each well was measured at 490 nm using a microplate reader (Model 680, Bio-Rad Laboratories, California, USA) under ambient conditions. For ELISAs of PEG-B-47, the reaction solutions were diluted fourfold prior to the measurements. The measured absorbance values were subjected to subtraction of the absorbance values obtained without cello-oligosaccharides. The experiments were performed at least in triplicate to obtain the average value and standard deviation.

To evaluate the effects of Tween 20, dispersions of the mEG_7-conjugated nanosheets with a 7% conjugation rate after incubation with 15-2b were similarly washed three times with PBS containing Tween 20. Subsequently, a washing cycle was preformed using PBS without Tween 20. Other procedures were performed in the same manners as described above. The measured absorbance values are shown without subtraction. The experiments were performed in triplicate to obtain the average value and standard deviation.

ELISAs were similarly performed at final anti-PEG antibody concentrations of 0.5–200 ng mL^{-1}, where anti-PEG antibodies were incubated with the OEG-conjugated nanosheets in the presence of 10% or 40% fetal bovine serum. The absorbance values of 100 μL of the reaction solutions were measured and shown without subtraction. The experiments were performed in triplicate to obtain the average value and standard deviation.

All-atom molecular dynamics (MD) simulation

According to the procedure in our previous study on all-atom MD simulations of celloheptaose assembly and hexylated celloheptaose assembly,[5] all-atom MD simulations were

performed using the MD program GROMACS 2024 for mEG_7-conjugated cellooctaose assemblies with mEG_7 conjugation rates of 8%, 25%, and 50% in water. In the initial structure of the system, a monolayer lamellar assembly was placed in the middle of the simulation box. The size of the box with periodic boundary conditions was (x, y, z) = (8.1000 nm, 8.0386 nm, 13.8000 nm). The remaining space in the simulation box was filled with water molecules. The numbers of propargylated cellooctaose molecules, mEG_7-bearing cellooctaose molecules, and water molecules are listed in Table S12.

The generalized Amber force field parameters[6] were adopted for propargylated cellooctaose and mEG_7-bearing cellooctaose molecules. TIP4P-Ew[7] was adopted for water molecules. The partial atomic charges of the propargylated cellooctaose and mEG_7-bearing cellooctaose molecules were calculated using the restrained electrostatic potential method based on DFT calculations (B3LYP/6–31 G(d)) using the GAUSSIAN 16 revision C.02 program.

After the steepest energy minimization, the pre-equilibration was run under the conditions: 2 ns at 298 K and 1 bar using the Berendsen thermostat and barostat[8] with relaxation times of 0.2 and 2.0 ps, respectively. The equilibration was run under the conditions: 30 ns at 298 K and 1 bar using the velocity rescaling thermostat[9] and the Parrinello-Rahman barostat[10] with relaxation times of 0.2 and 5.0 ps, respectively. Subsequently, an extended simulation with a time of 1 ns under the same conditions as the equilibration run was performed to analyze distance between the terminus of the mEG_7 chain and the grafting surface. The time step was set to 2 fs. All bonds connected to the hydrogen atoms were constrained with the LINCS algorithm.[11] The long-range Coulomb interactions were calculated using the smooth particle-mesh Ewald method[12] with a grid spacing of 0.30 nm. The real space cutoff for both the Coulomb and van der Waals interactions was 1.2 nm.

General techniques for characterization of organic synthesized compounds

NMR spectra were obtained using an AVANCE III HD500 instrument (500 MHz, Bruker Biospin, Massachusetts, USA) in the indicated solvent. Chemical shifts were shown in parts per million (ppm), and the residual solvent peak was used as an internal reference. ^{1}H NMR spectral data were referenced as follows: $CDCl_3$ (7.26 ppm) and methanol-d_4 (3.31 ppm). Multiplicities were identified as follows: s, singlet; d, doublet; t, triplet; dd, doublet of doublets; m, multiplet; *J*, coupling constants in Hertz.

Synthetic scheme for propargyl *β*-D-glucopyranoside

Propargyl *β*-D-glucopyranoside was synthesized as shown in Scheme S1.

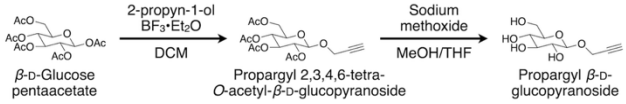

Scheme S1. Synthetic scheme of propargyl *β*-D-glucopyranoside.

Characterization data

Propargyl 2,3,4,6-tetra-*O*-acetyl-*β*-D-glucopyranoside. ^{1}H NMR (500 MHz, $CDCl_3$) δ 5.25 (t, 1H, *J* = 9.5, 9.5 Hz), 5.11 (t, 1H, *J* = 10.0, 10.0 Hz), 5.02 (t, 1H, *J* = 8.5, 9.0 Hz), 4.78 (d, 1H, *J* = 8.0 Hz), 4.38 (s, 2H), 4.28 (dd, 1H, *J* = 4.5, 12.0 Hz), 4.15 (d, 1H, *J* = 12.0 Hz), 3.73 (d, 1H, *J* = 10.5 Hz), 2.47 (s, 1H), 2.09 (s, 3H), 2.06 (s, 3H), 2.03 (s, 3H), 2.01 (s, 3H).

Propargyl *β*-D-glucopyranoside. ^{1}H NMR (500 MHz, methanol-d_4) δ 4.48–4.41 (m, 3H), 3.87 (d, 1H, *J* = 12.0 Hz), 3.66 (dd, 1H, *J* = 5.0, 12.0 Hz), 3.38–3.28 (m, 3H), 3.20 (t, 1H, *J* = 8.0, 9.0 Hz), 2.86 (s, 1H).

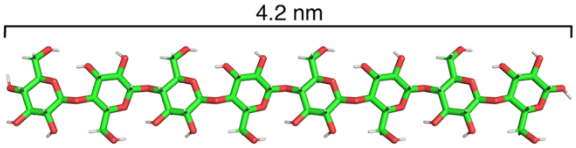

Fig. S1 A stick model of cellooctaose in the cellulose II allomorph.[2]

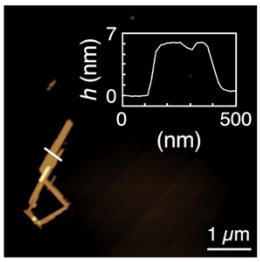

Fig. S2 AFM image for another batch of propargylated nanosheets.

Table S1 Conditions of copper(I)-catalyzed azide-alkyne cycloaddition reactions.

Conjugation rate of OEG chain (%)	[Propargylated cello-oligosaccharide assembly] (mg mL^{-1})	[Azidated OEG] (mM)	[Copper(II) sulfate] (mM)	[Sodium ascorbate] (mM)
7–10	2	2	0.5	0.2
21	2	4	1.0	0.4
55	2	6	1.5	0.6
75	2	8	2.0	0.8

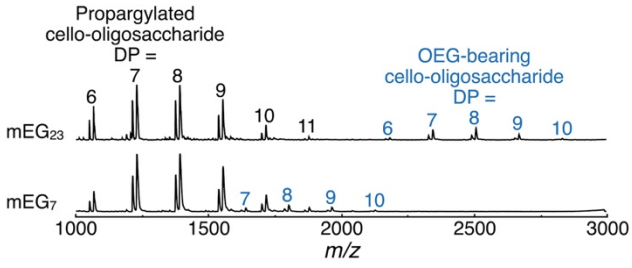

Fig. S3 MALDI-TOF mass spectra for another batch of the mEG_7-conjugated nanosheets and another batch of the mEG_{23}-conjugated nanosheets.

Table S2 Conjugation rate of OEG for another batch of OEG-conjugated nanosheets.

OEG-conjugated nanosheet	mEG_7-conjugated nanosheet	mEG_{23}-conjugated nanosheet
Conjugation rate for another batch	7%	12%
Conjugation rate for the batch presented in Table 1	7%	10%

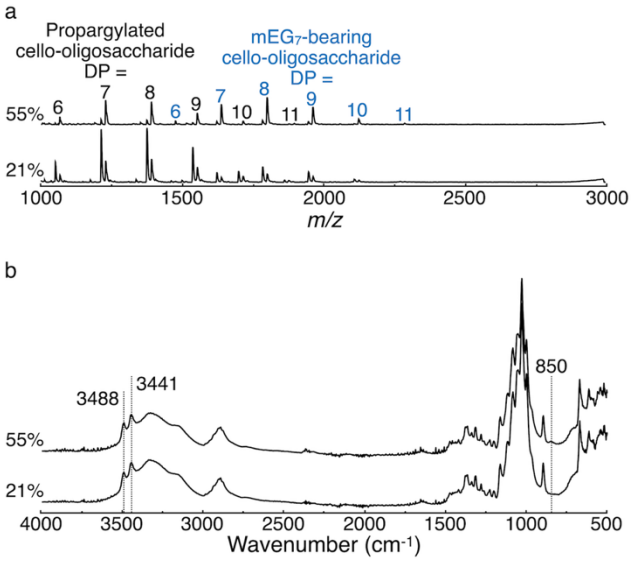

Fig. S4 (a) MALDI-TOF mass spectra and (b) ATR-FTIR absorption spectra of the mEG_7-conjugated nanosheets with mEG_7 conjugation rates of 21% and 55%.

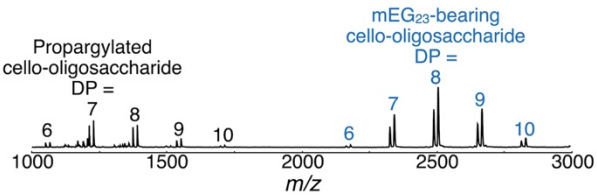

Fig. S5 MALDI-TOF mass spectrum of mEG_{23}-conjugated nanosheets with 75% conjugation rate.

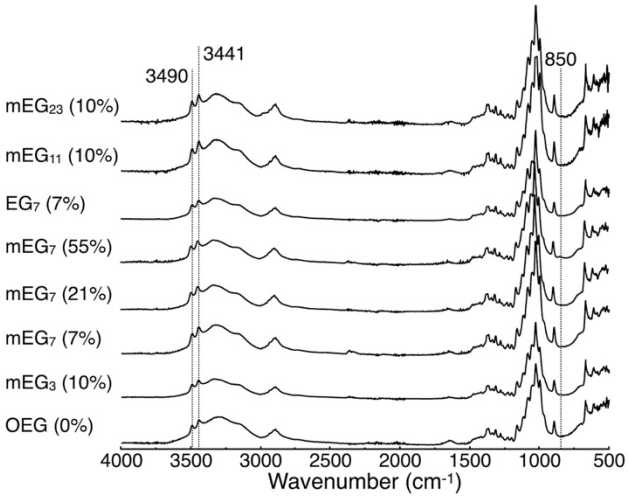

Fig. S6 ATR-FTIR absorption spectra of the propargylated nanosheets (denoted as OEG (0%)) and the OEG-conjugated nanosheets. The numbers in parentheses represent OEG conjugation rates.

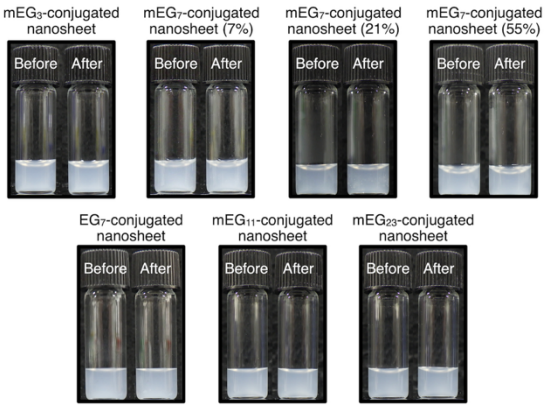

Fig. S7 Photographs of the dispersions of the OEG-conjugated nanosheets before and after 1 h incubation in PBS.

Table S3 Absorbance values from the ELISA results using the propargylated nanosheets, presented in Fig. 6a.

Clone	PEG-B-47	15-2b	6.3
Mean value ± standard deviation	0.015 ± 0.003	0.004 ± 0.010	0.002 ± 0.001

Table S4 Absorbance values from the ELISA results using the mEG_3-conjugated nanosheets, presented in Fig. 6b.

Clone	PEG-B-47	15-2b	6.3
Mean value ± standard deviation	1.166 ± 0.015	0.019 ± 0.009	0.021 ± 0.001

Table S5 Absorbance values from the ELISA results using the mEG_7-conjugated nanosheets, presented in Fig. 6c.

Clone	PEG-B-47	15-2b	6.3
Mean value ± standard deviation	1.114 ± 0.167	0.872 ± 0.027	0.022 ± 0.003

Table S6 Absorbance values from the ELISA results using the EG_7-conjugated nanosheets, presented in Fig. 6d.

Clone	PEG-B-47	15-2b	6.3
Mean value ± standard deviation	0.069 ± 0.006	0.024 ± 0.024	0.003 ± 0.002

Table S7 Absorbance values from the ELISA results using the mEG_{11}-conjugated nanosheets, presented in Fig. 6e.

Clone	PEG-B-47	15-2b	6.3
Mean value ± standard deviation	1.646 ± 0.054	1.397 ± 0.029	0.037 ± 0.007

Table S8 Absorbance values from the ELISA results using the mEG_{23}-conjugated nanosheets, presented in Fig. 6f.

Clone	PEG-B-47	15-2b	6.3
Mean value ± standard deviation	1.590 ± 0.064	1.762 ± 0.110	0.202 ± 0.063

Table S9 Absorbance value from ELISA result in the absence of anti-PEG antibody. HRP-conjugated anti-rabbit IgG antibody is used for PEG-B-47 ELISAs. HRP-conjugated anti-mouse IgG antibody is used for 15-2b and 6.3 ELISAs.

Nanosheet	OEG conjugation rate (%)	Absorbance value for HRP-conjugated anti-rabbit IgG antibody	Absorbance value for HRP-conjugated anti-mouse IgG antibody
Propargylated nanosheet	–	-0.003 ± 0.004	0.006 ± 0.012
mEG_3-conjugated nanosheet	10	-0.002 ± 0.002	0.012 ± 0.002
mEG_7-conjugated nanosheet	7	0.001 ± 0.001	0.010 ± 0.003
EG_7-conjugated nanosheet	7	-0.007 ± 0.002	-0.003 ± 0.006
mEG_{11}-conjugated nanosheet	10	0.005 ± 0.004	0.012 ± 0.003
mEG_{23}-conjugated nanosheet	10	0.002 ± 0.004	0.011 ± 0.002

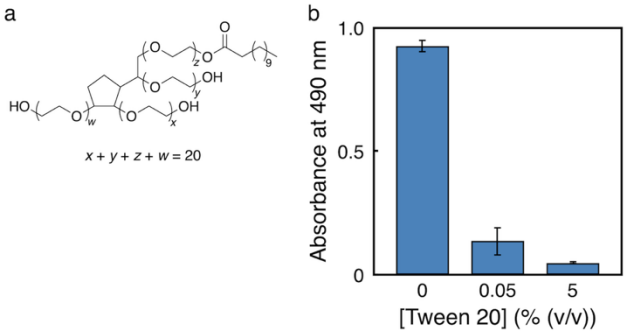

Fig. S8 (a) Chemical structure of Tween 20. (b) ELISAs of 15-2b using the mEG_7-conjugated nanosheets with 7% conjugation rate and PBS containing Tween 20 as a washing solution. The data is presented as mean ± standard deviation.

Table S10 Absorbance value from the ELISA result for 15-2b using another batch of mEG_{23}-conjugated nanosheets.

mEG_{23} conjugation rate	Mean value ± standard deviation of absorbance
12%	1.360 ± 0.125

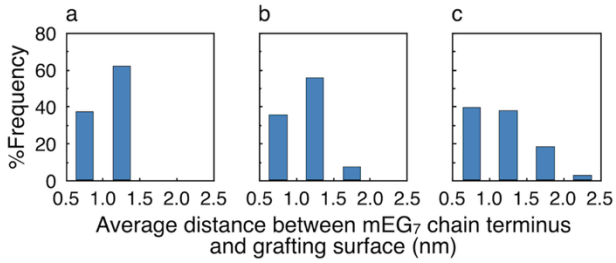

Fig. S9 Histograms of average distance between the terminus of mEG_7 chain and grafting surface during 1 ns extended simulations for the mEG_7-conjugated cellooctaose assemblies with mEG_7 conjugation rates of (a) 8%, (b) 25%, and (c) 50%.

Table S11 Structural properties of the mEG_8-conjugated cello-oligosaccharide nanosheets at a 100% conjugation rate.[4]

Average degree of polymerization value of cello-oligosaccharide moieties	Crystal allomorph	OEG chain	Flory radius (nm)	Distance between adjacent ligands (nm)
~11	Cellulose II	mEG_8	1.1	0.81 or 0.90

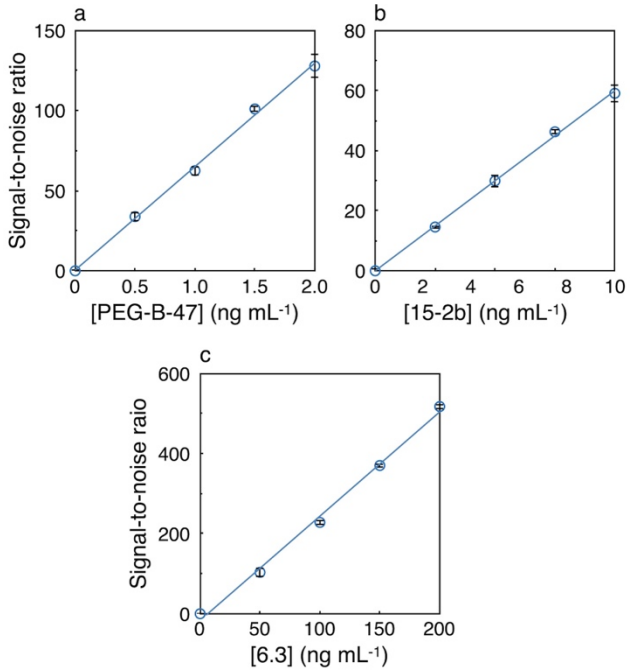

Fig. S10 Signal-to-noise ratios for ELISAs of (a) 0–2 ng mL^{-1} PEG-B-47 using 0.045% (w/v) mEG_3-conjugated nanosheets, (b) 0–10 ng mL^{-1} 15-2b using 0.045% (w/v) mEG_7-conjugated nanosheets, and (c) 0–200 ng mL^{-1} 6.3 using 0.045% (w/v) mEG_{23}-conjugated nanosheets in the presence of 10% fetal bovine serum. The lines denote linear fitting results. The data is presented as mean ± standard deviation.

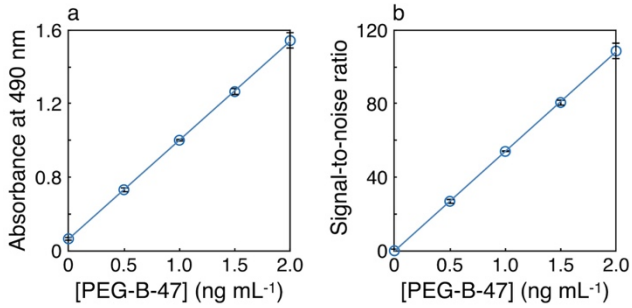

Fig. S11 (a) ELISA of 0–2 ng mL^{-1} PEG-B-47 in the presence of 40% fetal bovine serum using 0.045% (w/v) mEG_3-conjugated nanosheets and (b) signal-to-noise ratio for the ELISA. The lines denote linear fitting results. The data is presented as mean ± standard deviation.

Table S12 Distance between adjacent OEG chains and the number of the propargylated cellooctaoses, the mEG_7-bearing cellooctaoses, and the water molecules in the MD simulation box.

Conjugation rate (%)	Distance between adjacent OEG chains (nm)	Propargylated cellooctaose	mEG_7-bearing cellooctaose	Water
8	2.6 ± 0.3	184	16	19820
25	1.7 ± 0.1	150	50	19057
50	1.2 ± 0.3	100	100	17942

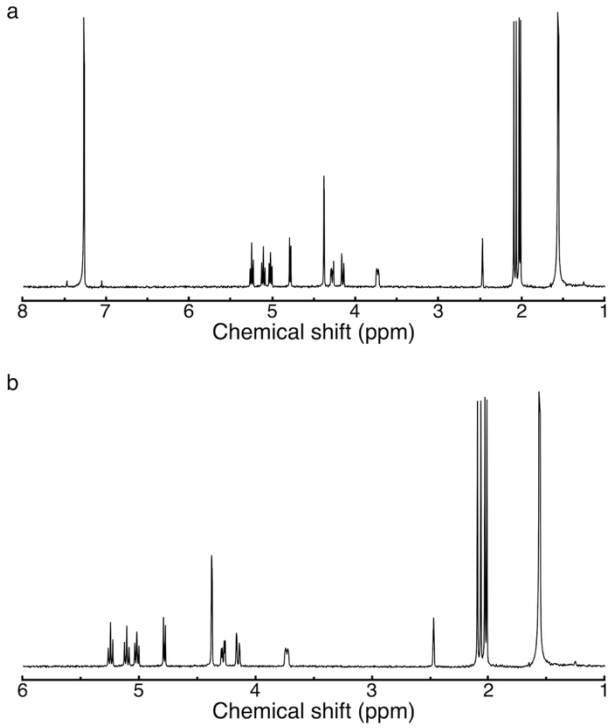

Fig. S12 ^{1}H NMR spectra (500 MHz, $CDCl_3$) of propargyl 2,3,4,6-tetra-*O*-acetyl-*β*-D-glucopyranoside in the range of (a) 1.0–8.0 ppm and (b) 1.0–6.0 ppm.

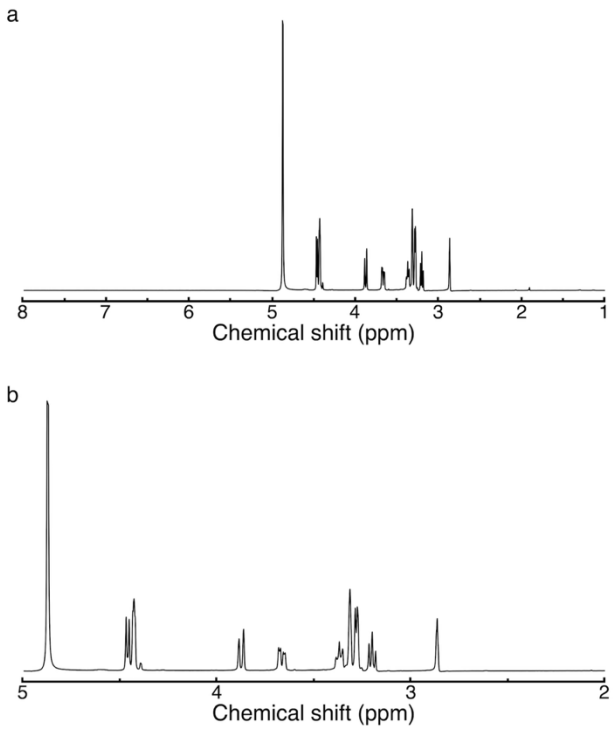

Fig. S13 ^{1}H NMR spectra (500 MHz, methanol-d_4) of propargyl *β*-D-glucopyranoside in the range of (a) 1.0–8.0 ppm and (b) 2.0–5.0 ppm.

References

1 T. Serizawa, S. Yamaguchi, K. Sugiura, R. Marten, A. Yamamoto, Y. Hata, T. Sawada, H. Tanaka and M. Tanaka, *ACS Appl. Bio Mater.*, 2024, **7**, 246–255.

2 P. Langan, Y. Nishiyama and H. Chanzy, *Biomacromolecules*, 2001, **2**, 410–416.

3 M. M. Hoffmann, R. H. Horowitz, T. Gutmann and G. Buntkowsky, *J. Chem. Eng. Data*, 2021, **66**, 2480–2500.

4 K. Sugiura, T. Sawada, Y. Hata, H. Tanaka and T. Serizawa, *J. Mater. Chem. B*, 2024, **12**, 650–657.

5 T. Serizawa, S. Yamaguchi, M. Amitani, S. Ishii, H. Tsuyuki, Y. Tanaka, T. Sawada, I. Kawamura, G. Watanabe and M. Tanaka, *Colloids Surf. B*, 2022, **220**, 112898.

6 J. Wang, R. M. Wolf, J. W. Caldwell, P. A. Kollman and D. A. Case, *J. Comput. Chem.*, 2004, **25**, 1157–1174.

7 H. W. Horn, W. C. Swope, J. W. Pitera, J. D. Madura, T. J. Dick, G. L. Hura and T. Head-Gordon, *J. Chem. Phys.*, 2004, **120**, 9665–9678.

8 H. J. C. Berendsen, J. P. M. Postma, W. F. van Gunsteren, A. DiNola and J. R. Haak, *J. Chem. Phys.*, 1984, **81**, 3684–3690.

9 G. Bussi, D. Donadio and M. Parrinello, *J. Chem. Phys.*, 2007, **126**, 14101.

10 M. Parrinello and A. Rahman, *J. Appl. Phys.*, 1981, **52**, 7182–7190.

11 B. Hess, H. Bekker, H. J. C. Berendsen and J. G. E. M. Fraaije, *J. Comput. Chem.*, 1997, **18**, 1463–1472.

12 U. Essmann, L. Perera, M. L. Berkowitz, T. Darden, H. Lee and L. G. Pedersen, *J. Chem. Phys.*, 1995, **103**, 8577–8593.